

This document is downloaded from DR-NTU, Nanyang Technological University Library, Singapore.

Title	Q-switched neodymium-doped Y3Al5O12-based silica fiber laser
Author(s)	Yoo, Seongwoo; Webb, A. S.; Standish, R. J.; May-Smith, T. C.; Sahu, Jayanta Kumar
Citation	Yoo, S., Webb, A. S., Standish, R. J., May-Smith, T. C., & Sahu, J. K. (2012). Q-switched neodymium-doped Y 3Al 5O 12-based silica fiber laser. Optics Letters, 37(12), 2181-2183.
Date	2012
URL	http://hdl.handle.net/10220/10956
Rights	© 2012 Optical Society of America. This paper was published in Optics Letters and is made available as an electronic reprint (preprint) with permission of Optical Society of America. The paper can be found at the following official DOI: [http://dx.doi.org/10.1364/OL.37.002181]. One print or electronic copy may be made for personal use only. Systematic or multiple reproduction, distribution to multiple locations via electronic or other means, duplication of any material in this paper for a fee or for commercial purposes, or modification of the content of the paper is prohibited and is subject to penalties under law.

Q-switched neodymium-doped $Y_3Al_5O_{12}$ -based silica fiber laser

S. Yoo,¹ A. S. Webb,² R. J. Standish,² T. C. May-Smith,² and J. K. Sahu^{2,*}

¹School of Electrical and Electronic Engineering, Nanyang Technological University, 639798 Singapore

²Optoelectronics Research Centre, University of Southampton, Southampton SO17 1BJ, UK

*Corresponding author: jks@orc.soton.ac.uk

Received February 14, 2012; revised April 13, 2012; accepted April 15, 2012;

posted April 16, 2012 (Doc. ID 163047); published June 4, 2012

We present pulsed laser operation in a Nd-doped, $Y_3Al_5O_{12}$ -based silica fiber. The fiber was fabricated using the rod-in-tube technique with a Nd:YAG crystal rod as the core material and a silica tube for the cladding material. A spectroscopy study revealed that the core region had become amorphous in the process of fiber drawing. Q-switched pulsed laser operation was realized at a wavelength of 1058 nm when the fiber was cladding pumped at a wavelength of 808 nm. The laser delivered 38 μ J of energy in 65 ns pulses. The extracted energy was limited due to the multimodal operation of the fiber. Laser slope efficiency in continuous wave operation reached 52%. The spectroscopic properties of the fabricated fiber are discussed and compared to a Nd:YAG crystal and a Nd:Al-doped silica fiber. © 2012 Optical Society of America

OCIS codes: 060.2290, 060.3510.

The dramatic progress in the achievable output power from fiber lasers has been made possible by the emergence of large-mode-area (LMA) fiber designs and the availability of high brightness pump diodes. The high output powers in LMA fibers are achieved by increasing the mode field diameter in order to overcome the detrimental effects of nonlinear interactions in the fiber core. Traditionally, high-power fiber sources use silica as a base material. Although rare earth (RE) doped silica fibers perform well in terms of scalability of the LMA design, the limited choice of codopants that can be incorporated into the silica matrix restricts the extent to which the optical properties can be manipulated (e.g. emission, transmission, and spectroscopic characteristics of the RE ions). In addition, the attainable level of RE ion concentration in the fiber is constrained by the silica host, as high concentrations cause RE clustering effects. However, a fiber structure that combines a non-silica rich core and silica cladding (hereafter called the “hybrid fiber”), can be used to manipulate the optical properties and relax the restriction on RE concentration. Hybrid fiber has been demonstrated with semiconductor core/silica cladding [1], non-silica core/silica cladding [2–4], YAG core/silica cladding [5–9], and silicate glass [10]. Despite several reports describing the fabrication of these fibers, there are limited results on interesting optical properties such as stimulated Brillouin scattering [11] or device works [7–9], and works on the pulsed operation of a hybrid fiber were initiated very recently in an amplifier configuration [9].

Here, we report the first demonstration of Q-switched laser operation in a cladding-pumped fiber with a Nd:YAG derived core and a silica cladding. The rod-in-tube technique was used to fabricate the fiber; this involved inserting a Nd:YAG (1 at. %) crystal rod (diameter: 2.5 mm) in the center of a drilled and polished F300 silica rod (diameter: 24 mm; supplied by Heraeus). The assembled preform was subsequently drawn into fiber with an inner cladding diameter of 200 μ m, and coated with a low refractive index UV-cured polymer outer cladding to provide a high numerical aperture (NA) of 0.48 for the inner cladding (pump

guide). The resultant fiber had a core diameter of \sim 20 μ m and core NA of 0.47. The background loss in the fiber was 1.2 dB/m at a wavelength of 1285 nm when measured using a high resolution optical time-domain reflectometer in 10 m fiber. Energy dispersive x-ray analysis (EDX) was performed to quantify the core composition of the fabricated fiber. Figure 1 shows the EDX line scan profiles of elements Si, Al, Y, and O across the core and cladding regions. The micrograph obtained from scanning electron microscopy (SEM) of the fiber cross section is inset. The average composition measured in the central core region of the optical fiber in a 10 μ m core consisted of Al_2O_3 : 13.4 wt. %, Y_2O_3 : 22.6 wt. %, and SiO_2 : 61.3 wt. %, evaluated based on EDX results, indicating that diffusion of silica from the cladding tube into the core has occurred during the fiber drawing process. The Nd concentration in the core is below the detection limit of the EDX apparatus used.

The fluorescence spectra and the upper laser level lifetimes of Nd-doped hybrid fiber, Nd:YAG bulk crystal, and Nd:Al-doped silica fiber were measured for comparison. The Nd:Al-doped silica fiber was fabricated in-house using conventional modified chemical vapor deposition in combination with the solution doping technique. The measured fluorescence decay curves are shown in Fig. 2. The lifetime in the hybrid fiber is between that of the Nd:YAG crystal and Nd:Al-doped silica fiber, measuring

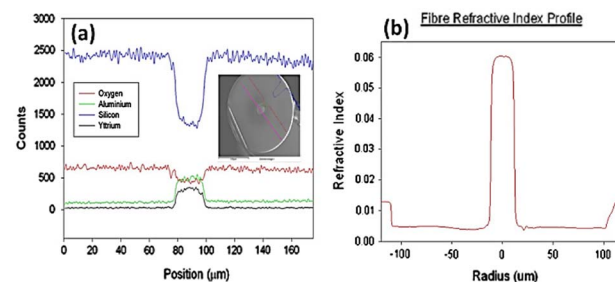


Fig. 1. (Color online) EDX line scan profiles (left) and refractive index profile (right) of fabricated fiber with SEM micrograph of fiber cross section (inset).

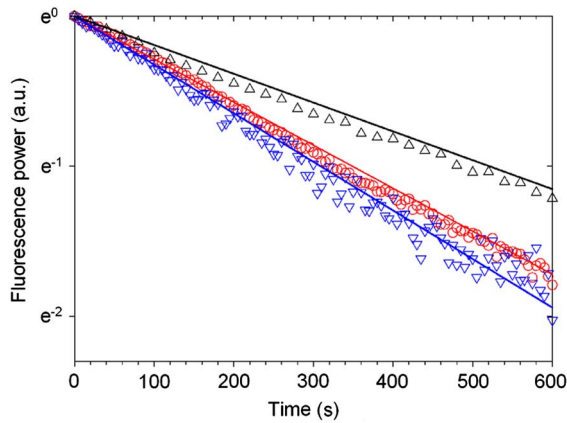


Fig. 2. (Color online) Fluorescence decay of Nd-doped hybrid fiber (red circles), Nd:Al-doped silica fiber (black triangles), and Nd:YAG crystal (blue inverted triangles). (Data points, experimental results; lines, exponential decay best fit).

330 μs , compared to 260 and 490 μs for the Nd:YAG crystal and Nd:Al-doped silica fiber respectively. The reduced lifetime in the hybrid type fiber from the silica fiber counterpart was observed elsewhere [7–9]. The upper laser level lifetimes and the fluorescence spectra were measured using an optical spectrum analyzer with 0.2 nm resolution. The data was then used to determine the emission cross section from the Füchtbauer–Ladenburg relation [12]. The emission cross section of the hybrid fiber is shown in Fig. 3 along with that of the Nd:Al-doped silica fiber and the Nd:YAG crystal. The peak emission cross section is $1.9 \times 10^{-24} \text{ m}^2$ at a wavelength of 1058 nm, compared to $1.6 \times 10^{-24} \text{ m}^2$ for the Nd:Al-doped silica fiber at the same wavelength. The broad emission spectrum of the Nd:YAG-derived hybrid fiber is indicative of the amorphous nature of the core. The crystal possesses a higher peak emission cross-section by one order of magnitude than the fiber counterparts, and it peaks at a slightly longer wavelength of 1063 nm. The Nd concentration of the Nd:Al fiber was determined as 1200 ppm-wt. The hybrid fiber is expected to have higher Nd concentration based on our calculation following the cladding absorption measurement [13]. The higher concentration of the hybrid fiber can be partly responsible for reduced lifetime, but fast decay component was not observed in 5 μs system response.

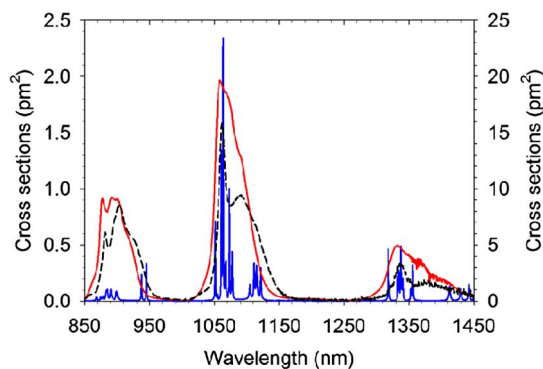


Fig. 3. (Color online) Measured emission cross section of Nd-doped hybrid fiber (red, left vertical axis), Nd:Al-doped silica fiber (black dashed curve, left vertical axis), and Nd:YAG crystal (blue with sharp peak, right vertical axis).

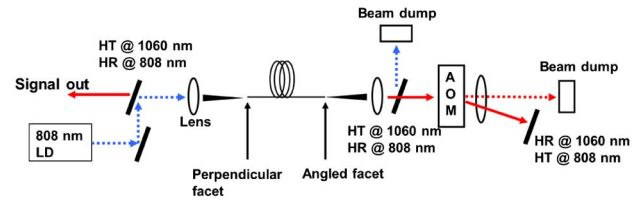


Fig. 4. (Color online) Experimental arrangement for Q-switched Nd-doped hybrid fiber laser.

The experimental setup used for the cladding pumped Q-switched Nd-doped hybrid fiber laser is shown in Fig. 4. The fiber was end-pumped by a multimode fiber pigtailed laser diode operating at a wavelength of 808 nm. The fiber inner cladding was circular. The pump beam was launched into the inner-cladding of the hybrid fiber using an optical configuration consisting of an aspheric lens, a reflective mirror, and a dichroic mirror which exhibited high transmissivity at the laser signal wavelength and high reflectivity at the pump wavelength. The pump input end was flat-cleaved to provide a 4% Fresnel reflection to the laser cavity. The other end of the fiber was angle-cleaved at 20° (considering the high core NA) to suppress unwanted feedback, and the cavity was completed by a dichroic mirror with a high reflection at the laser signal wavelength. An acousto-optic modulator (AOM) was introduced into the cavity for Q-switched operation. The first-order diffracted signal beam from the AOM was reflected back to the fiber by the dichroic mirror. The AOM permitted 90% of transmission at the laser signal wavelength. An energy meter was used to measure the pulse energy at a low repetition rate (below 1 kHz). Above a repetition rate of 1 kHz, the pulse energy was calculated by dividing the measured average power by the repetition rate. The contribution from amplified spontaneous emission (ASE) was subtracted from the total power measured with a thermal power meter to correctly record the average power.

Figure 5 shows the pulse energy and average power vs. repetition rate. The fiber length was 1.9 m, which permitted 8 dB of pump absorption. The pump power was adjusted to maximize the peak energy at a repetition rate of 1 kHz. The lasing wavelength was 1058 nm, which is consistent with the peak of the emission cross section. The slope with the AOM constantly on was 40% with respect to the absorbed pump power. The slope efficiency,

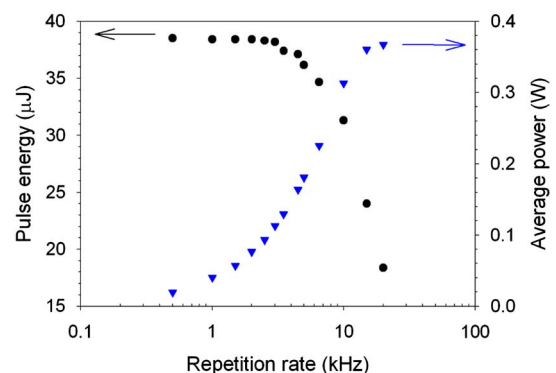


Fig. 5. (Color online) Laser pulse energy and average power versus repetition rate.

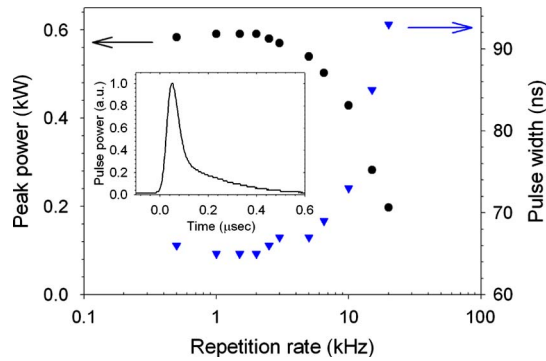


Fig. 6. (Color online) Peak power and pulse width versus repetition rate. Inset: temporal pulse shape.

however, was measured as 52% in a 4%–100% linear cavity without the AOM. The pulse energy increased as the repetition rate decreased, and reached a maximum of $38 \mu\text{J}$ at 3 kHz, whereas the average power increased as the repetition rate increased, which is typical for a Q-switched laser. The ASE buildup time was recorded as $125 \mu\text{s}$, which indicates that the ASE power can be significant, even at a relatively high repetition rate of 8 kHz. In fact, the ASE power takes 50% of the total power at 5 kHz. The high proportion of the ASE power is mainly attributed to the highly multimodal nature of the fiber, which had a V-number of around 30. The highly multimodal signal beam also limited the diffraction efficiency of the AOM to $\sim 20\%$. In addition, the small core size was partly responsible for the fast buildup of the ASE [14]. The extractable energy was estimated in the fiber by approximating it to ten times that of the saturation energy. The measured cross section in Fig. 3 was used to calculate the saturation energy. The extractable energy was found to be 0.29 mJ. Thus, the laser performance could be significantly improved by optimizing the fiber design as well as the cavity design.

Figure 6 shows the dependence of peak power and pulse width on the repetition rate. The peak power shows a similar trend to that of the pulse energy, and reaches 0.59 kW at its maximum. The pulse width broadens from 65 to 93 ns within the range of repetition rates tested. The inset in Fig. 6 shows a pulse with duration of 65 ns at the full width half maximum measured with the laser operating at a repetition rate of 2 kHz.

In summary, we have demonstrated a Q-switched cladding pumped fiber laser with a Nd-doped yttrium-aluminum rich silica core and silica cladding hybrid fiber. The spectroscopic characteristics of the hybrid fiber revealed that the Nd:YAG single crystal used in the preform core was modified in the process of fiber drawing and became amorphous. We have obtained $38 \mu\text{J}$ of pulse energy with 65 ns pulse duration at a repetition rate of 3 kHz

when diode pumped at a wavelength of 808 nm. The central lasing wavelength at 1058 nm is consistent with the peak of the emission cross section measured in the fabricated fiber. The extractable energy, which was expected to be higher than the experimental results, was impaired by the highly multimodal nature of the gain medium; the fast ASE buildup time also compromised the laser performance. We expect to achieve higher laser pulse energies by optimizing the fiber structure and cavity design. The slope efficiency in a continuous wave operation was 52% with respect to the absorbed pump power. Introducing raised inner cladding to achieve single-mode operation is in the scope of our next step.

This work was supported by the Engineering and Physical Sciences Research Council (EPSRC) Centre for Innovative Manufacturing in Photonics EP/HO2607X/1.

References

1. J. Ballato, T. Hawkins, P. Foy, R. Stolen, B. Kokuoz, M. Ellison, C. McMillen, J. Reppert, A. M. Rao, M. Daw, S. R. Sharma, R. Shori, O. Stafstudd, R. R. Rice, and D. R. Powers, *Opt. Express* **16**, 18675 (2008).
2. N. Granzow, S. P. Stark, M. A. Schmidt, A. S. Tverjanovich, L. Wondraczek, and P. St. J. Russell, *Opt. Express* **19**, 21003 (2011).
3. D. Furniss, J. D. Shephard, and A. B. Seddon, *J. Non-Cryst. Solids* **213–214**, 141 (1997).
4. N. K. Goel, R. H. Stolen, S. Morgan, J.-K. Kim, D. Kominsky, and G. Pickrell, *Opt. Lett.* **31**, 438 (2006).
5. J. Ballato, T. Hawkins, P. Foy, B. Kokuoz, R. Stolen, C. McMillen, M. Daw, Z. Su, T. M. Tritt, M. Dubinskii, J. Zhang, T. Sananyan, and M. J. Matthewson, *J. Appl. Phys.* **105**, 053110 (2009).
6. Y. C. Huang, J. S. Wang, Y. K. Lu, W. K. Liu, K. Y. Huang, S. L. Huang, and W. H. Cheng, *Opt. Express* **15**, 14382 (2007).
7. C. C. Lai, K. Y. Huang, H. J. Tsai, K. Y. Hsu, S. K. Liu, C. T. Cheng, K. D. Ji, C. P. Ke, S. R. Lin, and S. L. Huang, *Opt. Lett.* **34**, 2357 (2009).
8. P. D. Dragic, J. Ballato, T. Hawkins, and P. Foy, *Opt. Mater.* **34**, 1294 (2012).
9. P. D. Dragic, Y.-S. Liu, J. Ballato, T. Hawkins, and P. Foy, *Proc. SPIE* **8237**, 82371E (2012).
10. L. Sun, S. Jiang, J. D. Zuegel, and J. R. Marcianite, *Opt. Lett.* **35**, 706 (2010).
11. P. Dragic, P.-C. Law, J. Ballato, T. Hawkins, and P. Foy, *Opt. Express* **18**, 10055 (2010).
12. W. L. Barnes, R. I. Laming, E. J. Tarbox, and P. R. Morkel, *IEEE J. Quantum Electron.* **27**, 1004 (1991).
13. S. Yoo, A. S. Webb, R. J. Standish, T. C. May-Smith, and J. K. Sahu, "5.4 W cladding-pumped Nd:YAG fiber laser," to be presented at the Conference on Lasers and Electro-Optics (2012).
14. J. A. Alvarez-Chavez, H. L. Offerhaus, J. Nilsson, P. W. Turner, W. A. Clarkson, and D. J. Richardson, *Opt. Lett.* **25**, 37 (2000).